

MuCoMiD: A Multitask Convolutional Learning Framework for miRNA-Disease Association Prediction

Thi Ngan Dong and Megha Khosla

dong.khosla@l3s.de

L3S Research Center,

Leibniz University Hannover

Germany

ABSTRACT

Growing evidence from recent studies implies that microRNA or miRNA could serve as biomarkers in various complex human diseases. Since wet-lab experiments are expensive and time-consuming, computational techniques for miRNA-disease association prediction have attracted a lot of attention in recent years. Data scarcity is one of the major challenges in building reliable machine learning models. Data scarcity combined with the use of precalculated hand-crafted input features has led to problems of overfitting and data leakage.

We overcome the limitations of existing works by proposing a novel multi-tasking convolution-based approach, which we refer to as MuCoMiD. MuCoMiD allows automatic feature extraction while incorporating knowledge from 4 heterogeneous biological information sources (interactions between miRNA/diseases and protein-coding genes (PCG), miRNA family information, and disease ontology) in a multi-task setting which is a novel perspective and has not been studied before. The use of multi-channel convolutions allows us to extract expressive representations while keeping the model linear and, therefore, simple. To effectively test the generalization capability of our model, we construct large-scale experiments on standard benchmark datasets as well as our proposed larger independent test sets and case studies. MuCoMiD shows an improvement of at least 5% in 5-fold CV evaluation on HMDDv2.0 and HMDDv3.0 datasets and at least 49% on larger independent test sets with unseen miRNA and diseases over state-of-the-art approaches. We share our code for reproducibility and future research at <https://git.l3s.uni-hannover.de/dong/cmtt>.

1 INTRODUCTION

Over the past decades, many associations between MicroRNA or miRNAs and diseases have been confirmed using biological experiments leading to the belief that miRNAs could be potential biomarkers in certain diseases such as cancers, immune-related diseases [4, 11, 14, 21, 29, 33, 38]. The miRNA is a highly conserved class of non-coding RNA with a length of approximately 22 nucleotides. At the lowest level, miRNAs act as a gene expression regulation factor. miRNAs can up-regulate or down-regulate genes and thus indirectly affect the transcription processes. At a more systematic level, as suggested in [15, 23, 28], miRNAs play a vital role in determining the cellular fate as they can regulate development, maturation, differentiation, and apoptosis of the cell, cell signaling, cellular interactions, and homeostasis. Therefore, besides unveiling

a deeper understanding of diseases' molecular pathogenesis, identifying potential associations between miRNAs and diseases can also help in the treatment and discovery of possible drug targets.

Owing to the significance of the problem and the time-consuming nature of biological experiments, recent years have seen an upsurge in machine learning approaches [6, 19, 22, 25, 39] for *predicting miRNA-disease associations*. Being successfully able to predict miRNA-disease associations can lead to information prioritisation in biological wet-lab experimentation, which will result in considerable time and cost savings. From a machine learning perspective, the problem of predicting miRNA-disease associations can be formulated as that of a *link prediction problem* in a bipartite graph, where miRNA and disease form the two sets of nodes. However, as is typical to many biomedical applications, a major challenge for building generalizable and eventually well-performing models for the miRNA-disease association prediction problem is *data scarcity* of miRNA-disease data. For example, the total number of miRNA and disease nodes (without any preprocessing and removal of duplicates) in the standard HMDD v2.0 [20] database are 495 and 383 respectively with a total of 5,430 associations (links). These networks are therefore not only small with respect to the nodes set but are also sparsely connected.

Data scarcity often leads to biased and non-generalizable models. Earlier attempts to address data scarcity rely on creating additional secondary features based on the initial feature set by computing intra-node similarities, e.g., miRNA functional similarity. So much so, that these secondary features that encode miRNA functional similarity are pre-computed and are even deposited in well-known databases like MISIM [35]. The first problem associated with using such similarity-based input features is that it is prone to overfitting because slight errors in the input features get amplified by the secondary features. Secondly, models based on secondary features cannot be used to predict new associations for a miRNA (or a disease), i.e., instances for which no prior disease (or miRNA) association information is available.

More worrying is the problem of *data leakage* when using pre-computed miRNA functional similarities indiscriminately from available databases. Dong and Khosla [5] finds that most of the existing works that employ pre-computed similarities in model building ignore the actual train/test split giving rise to *data leakage*. In other words, some of the associations which are to be tested by the model are already present in the association network that was used to compute the similarity features. Finally, the small dataset size for the miRNA-disease prediction task prohibits the utility of flexible and more expressive modern representation learning approaches.

Present work. We overcome the above limitations in the earlier literature by avoiding the creation of secondary features altogether. Instead, our approach attempts to address the data scarcity problem by integrating knowledge from multiple heterogeneous sources of information available for miRNA and diseases in addition to the miRNA-disease associations. Combining multiple data sources enables us to compensate for missing or unreliable information in any single data type leading to more reliable predictions. Our key contribution is to model the integration of heterogeneous knowledge sources into a common representation space that can be trained end-to-end using modern representation learning machinery.

To this end, we propose a **Multitask Convolutional neural network for miRNA-Disease association prediction**, which we refer to as MuCoMiD for brevity. MuCoMiD allows automatic feature extraction while incorporating knowledge from 4 heterogeneous biological information sources (interactions between miRNA/diseases and protein-coding genes (PCG), miRNA family information, and disease ontology) in a *multi-task setting*. Instead of encoding miRNA and disease in separate representation spaces as in previous works, we employ shared 2D convolutions to infer underlying patterns associated with a pair of miRNA-disease directly from raw input features. These convolution operations allow us to extract expressive representations without comprising the model simplicity. Overall we have an expressive linear model with non-linear activation only at the output layer. The employed architecture allows us to overcome the problem of loss of interpretability usually associated with non-linear models. Besides, we employ *adaptive loss balancing* techniques to fine-tune multi-task loss gradients. This allows us to utilize the full power of multi-task learning without resorting to exhaustive hyperparameter search.

We conduct an extensive evaluation of our approaches in comparison to earlier works on existing benchmark datasets retrieved from HMDD v2.0 [20] and HMDD v3.0 [9] databases. In addition to evaluating our approach on standard benchmark datasets, we construct and test on new and larger test sets. We finally present case studies for three specific diseases to showcase the utility of our approach in predicting the association of novel diseases for which no prior miRNA association information is available in the train set.

Our Contributions. To summarize, we make the following contributions.

- We model the miRNA-disease association prediction problem in a *multi-task setting* incorporating heterogeneous domain knowledge, which is a novel perspective and has not been studied before for the current problem.
- We construct four new larger test sets for testing in transductive (when miRNA and disease nodes in the test set are also present in the train set) and inductive settings (when the test set contains a number of new miRNA or disease nodes).
- We conduct large-scale experiments and case studies for three specific diseases to showcase the superiority of our approach. We release all the code and data used in this study for reproducibility and future research at <https://git.l3s.uni-hannover.de/dong/cmtt>.

2 PROBLEM STATEMENT AND RELATED WORK

The miRNA-disease association data can be represented using a bipartite graph $\mathcal{G}_{md} = (U, V, E)$ where U is the set of nodes representing miRNAs and V denotes the set of disease nodes. Each edge $e = (u, v) \in E$ denotes the association between the miRNA node u and disease node v . We are then interested in the following problem statement.

Problem statement. *Given the bipartite graph $\mathcal{G}_{md} = (U, V, E)$, we are interested in (i) predicting missing links among the given nodes (transductive setting) (ii) predicting new links for so far unseen novel miRNA or disease nodes (inductive setting).*

2.1 Related work

Existing computational approaches for miRNA-disease association prediction can be broadly grouped into three classes: *scoring-based*, *network topology* and *machine learning* based methods.

Assuming that the miRNA pairs linked to common diseases are functionally more related scoring based methods [31, 35] proposed scoring systems to prioritize miRNA-disease associations. A more sophisticated scoring scheme while integrating information from miRNA and disease similarity networks was proposed in [36]. Network based approaches [1, 2, 18] construct miRNAs and/or disease similarity networks and aims at efficiently transferring known miRNA-disease association labels between similar miRNAs and/or similar diseases in the network. Chen et al. [1] employ repeated random walks with restarts over the miRNA functional similarity network and prioritize candidate miRNA-disease associations using the final stable walk probability.

More closely related to our work is the third category of machine learning based methods. Approaches in this category mainly rely on using secondary or hand-crafted features to construct similarity networks from which latent node features are extracted using graph-based representation learning techniques. EPMDA [6] extracts edge perturbation-based features from the miRNA-disease heterogeneous network and then trains a Multilayer Perceptron regression model to prioritize miRNA-disease associations. NNMDA [37] combines information from five different miRNA similarities and two disease similarities to build a heterogeneous network for feature learning and association prediction. Ji et al. [10] incorporates information from multiple domains, for example, miRNA-lncRNA and miRNA-PCG interaction, miRNA-drug association, disease-lncRNA, disease-PCG association, disease-drug association, to build a heterogeneous information network for feature extraction. The graph-based features along with miRNA k-mer feature (calculated from the miRNA sequence) and disease semantic similarity are concatenated to form the input to a Random Forest classifier for association prediction.

Another line of works include NIMGCN [19] and DimiG [25] which propose end-to-end learning approaches in which graph convolution networks (GCNs)[16] are employed for extracting latent features of miRNA and disease nodes. Non-graph based approaches like DBMDA [39] extract latent features from input hand-crafted features consisting of miRNA functional, disease semantic, and miRNA sequence similarity using autoencoders. The latent features are then fed to a Rotation Forest [27] classifier.

The reliance on hand-crafted features based on existing association data limits the applicability of existing techniques to transductive settings. Hence, apart from other limitations with respect to model generalization and data leakage (already discussed in Section 1) a majority of these approaches cannot be applied to predict associations for new miRNA or disease nodes that have not been observed in training data.

3 OUR APPROACH

To overcome the challenges of data scarcity, we propose MuCoMiD in which we focus on *effectively integrating heterogeneous biological information while learning to predict missing or new miRNA-disease associations*. MuCoMiD (also depicted in Figure 1) consists of three main modules: (i) *input graph construction*, (ii) *convolution based feature extraction*, and (iii) *multi-task optimization/learning*.

3.1 Input graph construction

We start by describing the construction or retrieval of various biological networks that we leverage as additional sources of information and the corresponding rationale.

Interaction networks, \mathcal{G}_{mp} and \mathcal{G}_{dp} . Protein coding genes (PCG) are believed to mediate associations between miRNAs and diseases [24]. For example, miRNAs can affect the regulation of protein-coding genes resulting in reduced or increased gene expression, which can then affect the pathology of a disease.

We obtain the miRNA-PCG interactions from the RAIN database [12]. We include only interactions for the PCGs with at least one associated Reactome pathway [7] as these would be biologically more significant. We then construct a bipartite network \mathcal{G}_{mp} in which the miRNA and PCGs form the set of nodes. An edge exists between miRNA and disease if there is a known interaction. We build a weighted adjacency matrix, A_{mp} , where the weight w_e corresponding to an edge e is equal to the normalized confidence score of the interaction, represented by e . $A_{mp}[i]$ then is used as the raw input feature vector for i th miRNA node.

We obtain the disease-PCG associations from the DISEASES database [26]. Here also, we retain only the associations for the PCGs with at least one associated Reactome pathway. As above, we construct the bipartite network, \mathcal{G}_{dp} with the node set consisting of diseases and PCGs. The normalized confidence scores of the corresponding interactions are used to construct the weighted adjacency matrix, A_{dp} . We use $A_{dp}[i]$ as input feature vector for the i th disease.

miRNA family, \mathcal{G}_m . A miRNA family is the group of miRNAs that share a common ancestor in the phylogenetic tree. miRNAs that belong to the same family usually have highly similar sequences, secondary structures and tend to execute similar biological functions [13]. Similar miRNA would tend to participate in the mechanisms of similar diseases. We retrieve miRNA family information from mirBase database [17]. We incorporate the miRNA family information into our model by optimizing a self-supervised learning objective designed on the structure of the family graph.

Disease ontology, \mathcal{G}_d . The disease ontology [30] represents the disease etiology classes. A directed connection between two diseases exists if there exists a **is-a** relationship between them. Similar

diseases can be expected to interact with similar miRNAs. The disease similarity is incorporated into the learning process via a graph-based self-supervised loss function defined on the structure of the disease ontology tree.

3.2 Convolution-based feature extraction

We learn an encoding of miRNA-miRNA, disease-disease, and miRNA-disease pairs in the same representation space using a shared 2D convolutional layer. For each miRNA/disease, the input is a feature vector of dimensions P where each element corresponds to a confidence score of interaction between the miRNA/disease and the corresponding PCG and P is the total number of PCGs. For each pair of input (miRNA-miRNA, miRNA-disease, or disease-disease), we then stack their input feature vectors vertically to form the input to a shared convolutional layer.

Let $\mathbf{X}_m \in \mathbb{R}^{P \times 2}$, $\mathbf{X}_d \in \mathbb{R}^{P \times 2}$, $\mathbf{X}_{md} \in \mathbb{R}^{P \times 2}$ denote inputs corresponding to pair of two miRNAs, pair of miRNA-disease, and pair of two diseases, respectively. Our 2D convolutional layer consists of $P/2$ output channels each with filter of size $P \times 2$. As our input is permutation invariant (since the order of elements in the input adjacency list does not matter), we use filters of size equal to the input size. Such an operation (as depicted in Figure 2) can be interpreted as learning multiple latent views of the data. Specifically, for a particular pair of inputs, convolution with each filter results in a weighted aggregation of all feature values where these weights are learned. These learned weights can be understood as the importance values of each of the features towards the latent views. In the following, we formulate the operations for an miRNA-disease pair. For other pairs, the operations are analogous. Let $\mathbf{x}_{md} \in \mathbb{R}^{P/2 \times 1}$ represents the output vector of the multichannel shared convolutional layer. Then

$$\mathbf{x}_{md}[i] = \mathbf{b}[i] + \sum_{j=0}^{P-1} \sum_{k=0}^1 \mathbf{W}_f[i, j, k] \cdot \mathbf{X}_m[j, k] \quad (1)$$

where $\mathbf{W}_f[i]$ and $\mathbf{b}[i]$ are the weight matrix and bias corresponding to the i th filter of the shared CNN layer, respectively. An illustration of the shared CNN operation is presented in Figure 2.

The shared CNN layer is responsible for learning the hidden pattern underlying the input pair's PCG interaction/association profiles. Each element in the output vector from the CNN layer represents a learned weighted sum of the input features (where each element is given a specific weight). The resulting vectors $\mathbf{x}'_m, \mathbf{x}'_{md}, \mathbf{x}'_d$ corresponding to miRNA-miRNA, miRNA-disease and disease-disease pairs respectively will be fed as input to corresponding task specific layer. To further fine tune latent pair representations we employ 3 separate linear task-specific layers, with parameters $\mathbf{w}_M \in \mathbb{R}^{P/2 \times 1}$, $\mathbf{w}_{MD} \in \mathbb{R}^{P/2 \times 1}$ and $\mathbf{w}_D \in \mathbb{R}^{P/2 \times 1}$.

The last module of our approach has further two sub-components: (i) multi-task loss functions and (ii) multi-task optimization using adaptive loss balancing. We describe the sub-components in the following sections.

3.3 Multi-task loss functions

We first describe the different loss functions employed for multi-task learning followed by our optimization strategy.

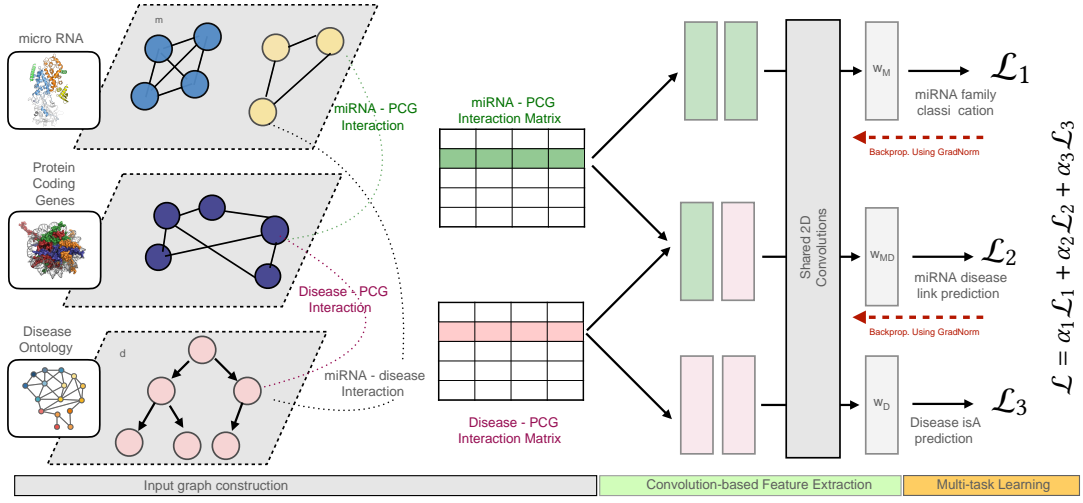


Figure 1: A schematic diagram of MuCoMiD. MuCoMiD consists of three main modules: (i) input graph construction in which we build bipartite networks corresponding to the available side information from miRNA family, interactions with PCG and disease ontology (ii) the second module uses miRNA-PCG and disease-PCG connectivity information and generates representations for each input pair (iii) finally, the losses are optimized in a multi-task framework using **GRADNORM**.

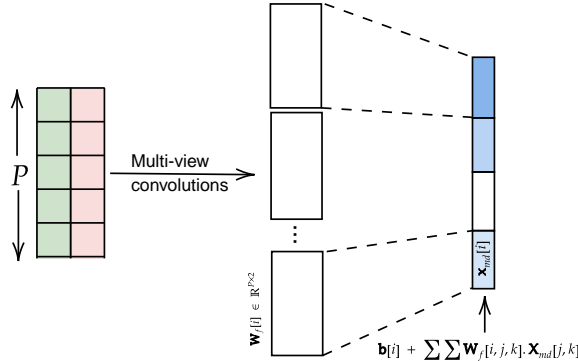


Figure 2: An illustration of the shared convolution operation.

Supervised loss for miRNA-disease association prediction. We compute the probability of a miRNA-disease association as

$$y_{md} = \sigma(\mathbf{w}_{MD}^T \mathbf{x}'_{md}) \quad (2)$$

where $\sigma(x) = \frac{1}{1+\exp(-x)}$ is the sigmoid function. We use binary cross entropy loss to train the miRNA-disease module.

$$\mathcal{L}_1 = \sum -z_{md} \log y_{md} - (1 - z_{md}) \log(1 - y_{md}) \quad (3)$$

We devise graph-based self-supervised objectives to incorporate topological information from the miRNA family graph and disease ontology tree.

Learning from disease ontology. For a given disease node, say d , we refer to the pair (d, d_p) as positive sample if nodes d and d_p are immediate neighbors in the ontology tree. For each positive sample, while keeping d fixed, we randomly draw k negative samples from

the h -hop away neighborhood distribution, \mathcal{P}_n . Specifically, we optimize the following graph based *self-supervised* objective for each edge (d, d_p) in \mathcal{G}_d

$$\log(\sigma(\mathbf{w}_D^T \mathbf{x}'_{dd})) + \sum_k \mathbb{E}_{d \sim \mathcal{P}_n} \log(\sigma(-\mathbf{w}_D^T \mathbf{x}'_{dd})) \quad (4)$$

The overall loss function is then given by

$$\mathcal{L}_2 = - \sum_{d, d} \left(\log(\sigma(\mathbf{w}_D^T \mathbf{x}'_{dd})) + \sum_k \mathbb{E}_{d \sim \mathcal{P}_n} \log(\sigma(-\mathbf{w}_D^T \mathbf{x}'_{dd})) \right) \quad (5)$$

Note that while we use the complete ontology tree \mathcal{G}_d to sample positive and negative examples, we retain pairs such that the corresponding PCG interaction information is available. In this study, we set k equal to 2.

Encoding similarity between miRNAs. To inform our model of miRNA similarity rather than using hand-crafted similarity features, we design a *self-supervised* objective on miRNA family clusters. Let the set of all clusters in \mathcal{G}_m is denoted by C . Let some miRNA, say m , belongs to cluster family $c \in C$. All pairs (m, m_p) , such that $m_p \in c$ constitute the positive pairs. For each such m , an equal number of negative samples are constructed by choosing pairs (m, m_n) such that $m_n \in C \setminus c$. Specifically, m_n is randomly sampled from a distribution over nodes not present in the current cluster. We denote this distribution as \mathcal{P}_n^M . We optimize the following loss function.

$$\mathcal{L}_3 = - \sum_{c \in C} \sum_{m, m \in c} \left(\log(\sigma(\mathbf{w}_M^T \mathbf{x}'_{mm})) + \mathbb{E}_{m \sim \mathcal{P}_n^M} \log(\sigma(-\mathbf{w}_M^T \mathbf{x}'_{mm})) \right) \quad (6)$$

3.4 Multi-Task optimization

We define the final loss for our model as the linear combination of three losses.

$$\mathcal{L} = \alpha_1 \mathcal{L}_1 + \alpha_2 \mathcal{L}_2 + \alpha_3 \mathcal{L}_3, \quad (7)$$

where $\alpha_1, \alpha_2, \alpha_3$ are loss weights corresponding to three loss functions. Generally, multi-task networks are difficult to train. Finding the optimal combination of individual task losses is challenging and problem-specific. To optimize model training, the contribution of each task needs to be balanced at each time step t . A task that is too dominant during training will overwhelm the update signals and prevent the network parameters from converging to robust shared features that are useful across all tasks.

We employ a gradient normalization technique (GRADNORM [3]) to adaptively find the best α_i for each training step t . The *adaptive loss balancing* approach allows us to find the best value of loss weights at each training step that balances the contribution of each task without resorting to exhaustive grid search procedures.

In particular, at a given time step t , GRADNORM defines a gradient norm

$$G_{\mathbf{W}}^{(i)}(t) = \|\mathbf{w} \alpha_i(t) \mathcal{L}_i(t)\|$$

as the L_2 norm of the gradient of the weighted single task loss $\alpha_i(t) \mathcal{L}_i(t)$ with respect to the parameters, \mathbf{W}_f , of the shared convolutional layer. We then define the gradient magnitude as the average gradient norm across all tasks:

$$\bar{G}_{\mathbf{W}f}(t) = \mathbb{E}_{\text{task}}[G_{\mathbf{W}}^{(i)}(t)].$$

Let $\mathcal{L}'_i(t) = \mathcal{L}_i(t)/\mathcal{L}_i(0)$ be the the loss ratio for the i th task at time t and

$$r_i(t) = \frac{\mathcal{L}'_i(t)}{\mathbb{E}_{\text{task}}[\mathcal{L}_i(t)]}$$

be the inverse relative training rate of task i . Higher $r_i(t)$ value implies higher gradient magnitude for task i and faster training for the corresponding task. The target gradient norm for each task i is given as:

$$G'^{(i)}(t) = \bar{G}_{\mathbf{W}f}(t) \times [r_i(t)]^\gamma$$

where γ is the additional hyper-parameter. Higher value of γ implies stronger training rate balancing. When tasks are more symmetric, a small value of γ is sufficient. In this work, we set the value of γ to be 0.5.

The task weight $\alpha_i(t)$ is updated so that the L_1 norm between the gradient norm $G^{(i)}(t)$ and the target gradient norm $G'^{(i)}(t)$:

$$\mathcal{L}_{\text{grad}}(t, \alpha_i(t)) = \sum_{i=1}^3 |G^{(i)}(t) - G'^{(i)}(t)|_1 \quad (8)$$

is minimized. $\mathcal{L}_{\text{grad}}$ is differentiated only with respect to loss weights $\alpha_i(t)$ as they directly control gradient magnitudes per task. The gradients are used to update loss weights using standard update rules. At each training step the loss weights are renormalized to decouple gradient normalization from the global learning rate.

4 EXPERIMENTAL SETUP

4.1 miRNA-disease association datasets

We retrieve the set of miRNA-disease associations from the HMDD v2.0 database [20] and HMDD v3.0 database [9]. As pre-processing

steps, we retain only associations for miRNAs and diseases for which the PCG interaction information is available. The filtered data for the HMDD v2.0 database, which from now on is denoted as HMDD2, contains 2,303 known associations between 368 miRNA and 124 diseases. The filtered data for the HMDD v3.0 database, which from now on is referred to as HMDD3, includes 8,747 known associations between 710 miRNAs and 311 diseases.

Table 1: The data statistics where $|E|, |V_{\text{miRNA}}|, |V_{\text{disease}}|$ refer to the number of associations/links, miRNAs and diseases respectively.

DATASET	$ E $	$ V_{\text{miRNA}} $	$ V_{\text{disease}} $
HMDD2	2,303	368	124
HMDD3	8,747	710	311

4.2 Statistics for additional biological networks

Table 2 provides statistics of biological networks that we constructed in Section 3.1. The networks are miRNA-PCG interaction network \mathcal{G}_{mp} , disease-PCG interaction network \mathcal{G}_{dp} , miRNA family network \mathcal{G}_{m} and disease ontology tree \mathcal{G}_{d} .

Table 2: Statistics for datasets with side information.

NETWORK	$ E $	$ V_{\text{miRNA}} $	$ V_{\text{disease}} $	$ V_{\text{PCG}} $
MIRNA-PCG (\mathcal{G}_{mp})	178,716	714	-	9,236
DISEASE-PCG (\mathcal{G}_{dp})	144,846	-	312	9,236
MIRNA FAMILY (\mathcal{G}_{m})	1,354	217	-	-
DISEASE ONTOLOGY (\mathcal{G}_{d})	90	-	128	-

4.3 Our new test sets

For small-size datasets like HMDD2 and HMDD3, 5-fold CV evaluation is limited as the size of the training and testing sets become much smaller. While one can use HMDD2 for training and HMDD3 for testing, such evaluation is limited as there are many overlapping associations in these two datasets. We, therefore, carefully construct the following four independent tests using the HMDD3 dataset. HMDD2 is used as the training set for evaluation with the new test sets.

Table 3: Statistics for our new test datasets.

DATASET	$ E $	$ V_{\text{miRNA}} $	$ V_{\text{disease}} $
HELD-OUT1	2,669	324	110
HELD-OUT2	6,641	692	303
NOVEL-MIRNA	3,575	577	115
NOVEL-DISEASE	5,308	346	295

HELD-OUT1 for transductive testing. We include in HELD-OUT1 the set of all miRNA, say M_2 , and disease nodes, say D_2 , which are in HMDD2. We only include those associations between M_2 and D_2 such that these are present in HMDD3 but not in HMDD2. This is

a transductive setting for link/association prediction such that all nodes in the testing set are the same as that in the training set. We randomly generate the same number of negative samples from the set of unknown miRNA-disease pairs. Finally, HELD-OUT1 contains 2,669 associations between 324 miRNAs and 110 diseases.

HELD-OUT2 for inductive testing. We construct the HELD-OUT2 test set by including miRNA-disease associations that are present in HMDD3 but not in HMDD2. Note that different from HELD-OUT1, HELD-OUT2 might also contain associations between miRNA and diseases which are not even present in the training set HMDD2. We randomly generate the same number of negative samples from the set of unknown miRNA-disease pairs. HELD-OUT2 consists of 6,641 associations between 692 miRNAs and 303 diseases.

NOVEL-miRNA. We first fix the set of diseases in our test set to those retained from HMDD2, i.e., the set D_2 . Then all known associations for the set D_2 which are present in HMDD3 but not in HMDD2 are included in the NOVEL-miRNA test set. We randomly generate the same number of negative samples from the set of unknown miRNA-disease pairs. In the end, our unseen miRNA testing set consists of 3,575 associations between 577 miRNAs and 115 diseases. We use this set to test the performance of models on unseen data where there are new miRNAs for which no prior association is present in the training set.

NOVEL-DISEASE. Similarly, for constructing the NOVEL-DISEASE test set, we first include the set of all miRNAs M_2 from HMDD2. Then we include the set of all associations and corresponding diseases which are in HMDD3 but not in HMDD2. We randomly generate the same number of negative samples from the set of unknown miRNA-disease pairs. Finally, we attain 5,308 associations between 346 miRNAs and 295 diseases. We use this set to test the performance of models on unseen data where there are new diseases for which no prior association is present in the training set.

4.4 Data for case studies

To further demonstrate our multi-task model’s predictive capability, we evaluate the model for three specific diseases: BREASTCANCER, PANCREATICCANCER, and DIABETESMELLITUS-type 2. By constructing these case studies, we showcase our model’s predictive performance in predicting associations for a specific new disease. To do that, for a specific disease d , we select the pairs associated with d from the HMDD3 to use as the testing set. The remaining pairs in HMDD3 are used as the training data. We do negative sampling for both the training and testing set so that the number of positive and negative samples in both training and testing sets are equal. For the test set, the negative pairs are generated only corresponding to the disease d . The dataset statistics for our case studies are presented in table 4 where we use the disease names to denotes our generated dataset for that particular disease case study.

4.5 Benchmarked models

We compare our model with five recently proposed supervised methods, and one multi-task baseline. Details about our benchmarked models are given below.

EPMDA [6] EPMDA consists of two components: the feature extractor and the classifier. The feature extraction module adopts

Table 4: Our case studies’ datasets’ statistics, where n^+ and n^- refer to the number of positive and negative associations/links, respectively.

DISEASE	TRAIN SAMPLES		TRAIN SAMPLES	
	n^+	n^-	n^+	n^-
BREASTCANCER	8423	8423	324	324
PANCREATICCANCER	8578	8578	169	169
DIABETESMELLITUS	8640	8640	107	107

a network topology-based approach and operates on a heterogeneous network G . G is constructed from the known miRNA-disease association set, the pre-calculated miRNA, and disease Gaussian Interaction Profile Kernel (GIP) [34] similarities. A Multiple Layer Perceptron (MLP) classifier is employed to do the classification task. EPMDA feature extractor and classifier get trained separately.

NEMII [8] NEMII uses Structural Deep Network Embedding (SDNE) to learn the embedding for miRNA and disease from a bipartite graph built up from known association information. The learned embedding and features extracted from the miRNA family and disease semantic similarity are concatenated to form the input to a Random Forest classifier.

NIMGCN [19] NIMGCN proposes an end-to-end learning framework that operates on a heterogeneous network G , which is built up from miRNA-disease known associations, the pre-calculated miRNA functional similarity (MISIM), and the disease semantic similarities. GCN and non-linear transformation layers are employed to learn the latent representation for miRNAs and diseases separately. For a particular miRNA-disease pair, its association probability is calculated as the inner product of the two corresponding latent feature vectors.

DBMDA [39]. DBMDA separates the feature learning and classification process. It uses autoencoders to learn the hidden representation for each miRNA-disease pair from pre-calculated similarities as input. The autoencoders are trained in an unsupervised manner. The encoded representation will then be fed as input into a Rotation Forest classifier whose job is to predict potential miRNA-disease associations.

DIMIG 2.0 [25] DIMIG 2.0 is a semi-supervised approach that treats miRNA-disease association prediction as a multiclass classification problem where diseases are the labels. They do not use miRNA-disease association during the training process. Instead, they use only the known disease-PCGs interaction to learn the model parameters. PCGs nodes are connected with miRNAs nodes in a heterogeneous network based on miRNAs interaction profiles. Learned signals are then propagated through the heterogeneous network to infer the labels for miRNAs.

Note that from all the above baselines, only DIMIG 2.0 can be used for testing in inductive settings, i.e., testing for associations/links when the corresponding nodes are not present in the train set. We, therefore, build another multi-task learning baseline specifically for inductive settings. As this baseline follows the multi-tasking based design principles of MuCoMiD and uses additional GCNs to learn node representations, we refer to it as GCN-MuCoMiD.

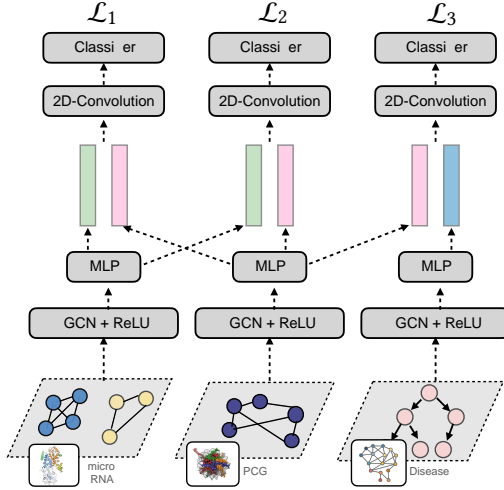


Figure 3: Architecture of our proposed GCN-MuCoMiD baseline. GCN-MuCoMiD like MuCoMiD is a multi-tasking approach but additional extracts initial node features using GCNs before generating a pair representation using task specific 2D convolutional layers. Additionally it leverages PCG interaction networks.

GCN-MuCoMiD. We construct, GCN-MuCoMiD, a multi-task baseline approach which is trained to predict miRNA-disease association, miRNA-PCG, and disease-PCG interaction confidence scores (formulated as regression tasks). An illustration of the GCN-MuCoMiD model is presented in figure 3. Regarding the sources of information, apart from those mentioned above, GCN-MuCoMiD incorporates additional information from the PCG-PCG interaction network. Interaction pairs along with their confidence scores are retrieved from STRING database [32]. The PCG network \mathcal{G}_p is an undirected weighted network in which the edge weights are the PCG pairs interaction confidence score retrieved from STRING.

Compared with MuCoMiD, GCN-MuCoMiD employs a more complex architecture with non-linear transformations. GCNs followed by Multiple Layer Perceptron (MLP) with ReLU activation layers are employed to extract the latent representation for miRNA, PCG, and disease nodes from miRNA family, PCG networks, and the disease directed acyclic graph (built up from the disease ontology) respectively. Similar to MuCoMiD, the pairwise node representations are then fed to the 2D convolutional layers to learn the underlying pair patterns. Finally, Logistic Regression (LR) layers are added to predict the miRNA-disease association probability and miRNA-PCG, disease-PCG interaction/association confidence score.

GCN-MuCoMiD multi-task loss function takes a similar form as MuCoMiD (which is given in equation 7). We employ *dynamic* task weighting techniques to fine-tune the multi-task loss gradients (since GRADNORM requires at least one shared layer between all tasks, which is not available in GCN-MuCoMiD architecture). More specifically, at each training epoch, the weight for task i is proportional with the fraction of its loss value compared to the sum of all tasks' losses, i.e., $\alpha_i = \mathcal{L}_i / \sum_{j=1}^3 \mathcal{L}_j$.

4.6 Test set-up and evaluation

As in previous works, we perform 5-fold CV for testing on HMDD2 and HMDD3 datasets. We run 5-fold CV with 5 random initializations. In other words, for each dataset, we run each model $5 \times 5 = 25$ times and report the average performance with the standard deviation.

To test on our new test sets, we train the models on the HMDD2 dataset. We run the experiments 5 times with random seed initializations and report the mean performance scores along with standard deviation. For case studies, we run each model with the given case study data 5 times and report average performance for each model.

Evaluation metrics. Following previous works and recommendations in [5], we report the Area under the Receiver Operating Characteristic (AUC), and Average Precision(AP) as our evaluation criteria. For our case studies, we report the number of known associations found in the top K results returned from the model, where k is from 10 to 100 with a step of 10.

4.7 Parameter set up

4.7.1 MuCoMiD. We set the output dimension for the convolutional layers to be half of the input dimension, i.e., equal to 4,618. The training rate balancing parameter γ is set to 0.5. The number of training epochs for HMDD3, independent testing sets, and case studies is set to 100. For 5FoldCV on HMDD2, we set the training epochs to 40. We employ Adam optimizer with a learning rate of 10^{-3} for training.

4.7.2 Benchmarked models. For EPMDA, DBMDA and NIMGCN, we use the code and setup released in [5]. For NEMII, we use the same code and setup as published by the authors.

For DIMIG 2.0, we use the code and parameters shared by the author. To test the model performance on our data, we compared DIMIG 2.0 with the input features as tissue expression profiles and DIMIG 2.0 with one-hot vectors on the subset of our testing datasets that have miRNA expression profiles available. The two models acquire similar performance. This implies that use of tissue expression profiles as node features do not have an effect on the model performance. We can therefore test the model on data for which tissue expression information is unavailable by using one hot encoding for input node features. The results reported in Section 5 corresponds to the model with one-hot vectors as input features on our testing datasets without removing miRNAs that don't have expression profiles.

For GCN-MuCoMiD, we set the training epochs to be 200 in all experiments. We use BinaryCrossEntropy to calculate the loss for miRNA-disease association prediction task and MeanSquaredError to calculate the loss for the other side tasks. Adam optimizer with a learning rate of 10^{-3} is employed to optimize the model parameters.

5 RESULTS

In the following, we discuss the performance gains of our approach (and their implications) on a variety of testing scenarios and new test datasets described in sections 4.1 and 4.3.

Table 5: Results with 5FoldCV over the HMDD2 and HMDD3 datasets. We perform 5-Fold CV 5 times with different random seeds. We report the average over 25 scores along with standard deviation. Our improvements over state-of-the-art (SOTA) methods are statistically significant with a p-value less than 0.002 on HMDD2 and less than 10^{-30} on HMDD3 datasets.

Method	HMDD2		HMDD3	
	AUC	AP	AUC	AP
EPMDA (Dong et al. [6])	0.744 ± 0.019	0.783 ± 0.017	0.520 ± 0.011	0.594 ± 0.010
NIMGCN (Li et al. [19])	0.785 ± 0.018	0.803 ± 0.015	0.795 ± 0.021	0.800 ± 0.018
DBMDA (Zheng et al. [39])	0.553 ± 0.019	0.537 ± 0.015	0.749 ± 0.010	0.696 ± 0.009
NEMII (Gong et al. [8])	0.499 ± 0.019	0.502 ± 0.020	0.512 ± 0.008	0.509 ± 0.006
DIMIG 2.0 (Pan and Shen [25])	0.493 ± 0.018	0.485 ± 0.012	0.516 ± 0.006	0.508 ± 0.005
MuCoMiD (ours)	0.841 ± 0.013	0.849 ± 0.014	0.917 ± 0.003	0.916 ± 0.005
GCN-MuCoMiD (ours)	0.825 ± 0.015	0.829 ± 0.017	0.851 ± 0.005	0.844 ± 0.007
Improvement over SOTA	7.1%	5.7%	15.3%	14.5%

5.1 Results on small test sets

Following previous works, we perform 5-fold CV experiments on HMDD2 and HMDD3 datasets. The results are shown in Table 5. The test set size for this scenario is considerably smaller and contains only 1/5th of the total associations. The test size is then considerably smaller for datasets like HMDD2. Such a train-test scenario allows us to quantify how well the models learn but is limited in testing the generalization power of the models.

While the graph-based approaches EPMDA and NIMGCN perform reasonably well in this scenario, our multi-task-based approaches significantly supersede state-of-the-art (SOTA) methods with an improvement of up to $\sim 14.5\%$ in AP score.

The performance of EPMDA drops considerably for HMDD3 dataset. EPMDA learns edge features in an unsupervised manner corresponding to its contribution to a cycle of a particular length. Usually, the cycle length parameter is fixed to a small value due to an exponential increase in run time with an increase in cycle length. Moreover, the task signal is not used in learning the edge features. The loss of performance of EPMDA in HMDD3 can be attributed to the limitation of finding the best cycle length hyperparameter applicable for HMDD3. This also limits the applicability of this model to a larger variety of datasets. NIMGCN performs better than DBMDA due to the higher representational capacity of used GCNs and exploitation of additional graph structure.

MuCoMiD outperforms our own GCN-based complex baseline for both these datasets. Due to the simplicity of MuCoMiD, the standard deviation in performance over different runs is also smaller than that observed for GCN-MuCoMiD. In general GCN-MuCoMiD also outperforms all state-of-the-art methods, which shows the superiority of our overall design principle of using a multi-tasking approach for joint learning from multiple data sources.

5.2 Results on small train but larger test sets in transductive setting

Table 6 shows results corresponding to HELD-OUT1 test set. Recall that HMDD2 is used as the training set. In this scenario, the test size is much larger than the train set size allowing us to compare the generalization capability of the models.

Table 6: Results on the HELD-OUT1 dataset after five runs. Our improvements over SOTA methods are statistically significant with a p-value less than 10^{-15} .

Method	AUC	AP
EPMDA	0.562 ± 0.085	0.511 ± 0.064
NIMGCN	0.676 ± 0.009	0.642 ± 0.006
DBMDA	0.545 ± 0.011	0.521 ± 0.009
NEMII	0.504 ± 0.002	0.501 ± 0.000
Dimig 2.0	0.429 ± 0.002	0.471 ± 0.003
MuCoMiD (ours)	0.706 ± 0.000	0.684 ± 0.000
GCN-MuCoMiD (ours)	0.711 ± 0.001	0.689 ± 0.003
Improvement over SOTA	4.4%	6.5%

Out of the state-of-the-art models, NIMGCN is the best owing to the use of GCNs to extract latent representations. The overall drop in performance of all models in this scenario as compared to small test size case points to the hardness of this particular test set. Existing methods show a bad generalization capability.

Our GCN-MuCoMiD is the best performing method and is closely followed by MuCoMiD. Nevertheless, MuCoMiD has a simpler architecture, and the performance difference is very small ($\sim 0.7\%$).

5.3 Results on small train but larger test sets in inductive setting

Table 7 shows results corresponding to testing on HELD-OUT2 dataset and training on HMDD2. Note that HELD-OUT2 is more than three times larger than the training data and contains new nodes not seen in HMDD2. EPMDA, DBMDA, NIMGCN, and NEMII rely on the known miRNA-disease associations to calculate similarities or learn structural embedding for miRNA and disease. Therefore, they cannot be compared in the current inductive setting with new miRNAs or new diseases.

For such large testing set with many new nodes, MuCoMiD still claims its superior performance. MuCoMiD is $\sim 14.2\%$ better in AP score compared to GCN-MuCoMiD. With respect to AP score, it shows an improvement of $\sim 59.1\%$ over Dimig 2.0.

Table 7: Results on large test sets with new miRNA and disease after five runs. Our improvements over SOTA methods are statistically significant with a p-value less than 10^{-15} . All models are trained on HMDD2 dataset.

Method	NOVEL-MiRNA		NOVEL-DISEASE		HELD-OUT2	
	AUC	AP	AUC	AP	AUC	AP
DIMIG 2.0	0.452 ± 0.001	0.480 ± 0.001	0.421 ± 0.001	0.467 ± 0.001	0.417 ± 0.003	0.465 ± 0.004
MuCoMiD	0.735 ± 0.000	0.715 ± 0.000	0.713 ± 0.000	0.707 ± 0.000	0.732 ± 0.000	0.740 ± 0.000
GCN-MuCoMiD	0.733 ± 0.005	0.712 ± 0.004	0.629 ± 0.006	0.622 ± 0.007	0.643 ± 0.006	0.648 ± 0.005
Improvement over SOTA	62.6%	49%	69.4%	51.4%	75.5%	59.1%

This dataset further supports the importance of the chosen architecture and the effectiveness of multi-sources data integration. MuCoMiD’s standard deviation among five runs is less than 10^{-3} . MuCoMiD not only obtains better mean performance scores than GCN-MuCoMiD but also shows lower standard deviation($<10^{-3}$) among different runs. The simple linear architecture of our model allows it to avoid overfitting. At the same time, the use of multi-channel convolutions to extract latent multi-view representations allows it to effectively exploit the side information.

5.4 Results on NOVEL-DISEASE and NOVEL-MiRNA datasets

Table 7 shows results with NOVEL-DISEASE and NOVEL-MiRNA test sets. EPMDA, DBMDA, NIMGCN, and NEMII cannot be used for inductive setting with new nodes.

MuCoMiD outperforms all baselines showing negligible variance over different runs. The gain is more significant on NOVEL-DISEASE datasets where the number of new diseases is nearly two times larger than the number of diseases observed in the training data. On NOVEL-DISEASE test set, MuCoMiD is $\sim 13.7\%$ and $\sim 69.4\%$ better in AP score than GCN-MuCoMiD and DIMIG 2.0, respectively. On NOVEL-MiRNA dataset, MuCoMiD acquires similar gain with respect to DIMIG 2.0 but is only slightly better than GCN-MuCoMiD.

5.5 Case studies

Figure 4 presents the topK evaluation results for three diseases. For each case study, the known association for that particular disease is completely hidden from the model training process. The statistics of our training and testing data can be found in Section 4.

Looking at Figure 4, though the case studies’ diseases are completely new, our model still attains perfect prediction for the top 40 predictions. Compared with DIMIG 2.0 for the top 50 predictions, our model has a gain of at least 177%.

For BREASTCANCER, the model acquires 100% accuracy for the top 100 predictions. For DIABETESMELLITUS-type 2, the number of known positive associations is 107, but out of the top 100 predictions, we can correctly recognize 91.2 associations (this number is the average of the number of found interactions over five runs).

6 CONCLUSION

We propose a multi-task convolutional learning framework, MuCoMiD for the problem of predicting miRNA-disease associations. Our end-to-end learning approach allows automatic feature extraction while incorporating knowledge from 4 heterogeneous biological information sources. While being a linear model, MuCoMiD

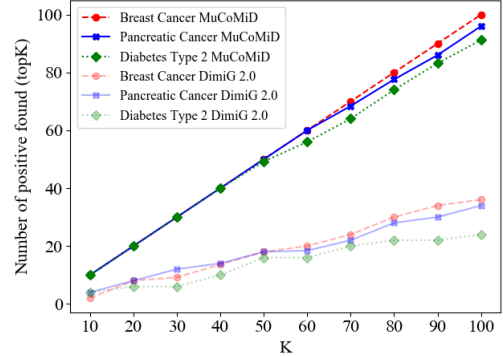


Figure 4: topK interactions for case studies. Mean number of interactions found over 5 independent runs of the models are reported.

enjoys high expressive power thanks to the multi-channel convolutions. Unlike previous works, our model can be employed in both transductive and inductive settings. To test the generalization power of models, we construct and test on larger test sets. Large-scale experiments in several testing scenarios highlight the superiority of our approach. We release all the code and data used in this study for reproducibility and future research at <https://git.l3s.uni-hannover.de/dong/cmtt>.

We believe that our design principles will be of independent interest for other biomedical applications where data scarcity is a major challenge. In particular, the use of multi-task learning to integrate information from heterogeneous information sources to overcome the problems of data scarcity and unreliability of one single data type is a unique perspective and has not been studied for computational problems in biomedicine.

ACKNOWLEDGMENTS

The first author is supported by project PRESENT funded by Volkswagen Stiftung and the State Government of Lower Saxony (grant no. 11-76251-99-3/19 (ZN3434)). The second author is supported by the Federal Ministry of Education and Research (BMBF), Germany under the project LeibnizKILabor (grant no. 01DD20003).

REFERENCES

[1] Xing Chen, Ming-Xi Liu, and Gui-Ying Yan. 2012. RWRMDA: predicting novel human microRNA–disease associations. *Molecular BioSystems* 8, 10 (2012), 2792–2798.

[2] Xing Chen, De-Hong Zhang, and Zhu-Hong You. 2018. A heterogeneous label propagation approach to explore the potential associations between miRNA and disease. *Journal of translational medicine* 16, 1 (2018), 348.

[3] Zhao Chen, Vijay Badrinarayanan, Chen-Yu Lee, and Andrew Rabinovich. 2018. Gradnorm: Gradient normalization for adaptive loss balancing in deep multitask networks. In *International Conference on Machine Learning*. PMLR, 794–803.

[4] Maurice WJ de Ronde, Jan M Ruijter, Perry D Moerland, Esther E Creemers, and Sara-Joan Pinto-Sietsma. 2018. Study design and qPCR data analysis guidelines for reliable circulating miRNA biomarker experiments: a review. *Clinical chemistry* 64, 9 (2018), 1308–1318.

[5] Thi Ngan Dong and Megha Khosla. 2020. Towards a consistent evaluation of miRNA-disease association prediction models. In *2020 IEEE International Conference on Bioinformatics and Biomedicine (BIBM)*. IEEE, 1835–1842.

[6] Yadong Dong, Yongqi Sun, Chao Qin, and Weigu Zhu. 2019. EPMDA: Edge perturbation based method for miRNA-disease association prediction. *IEEE/ACM Transactions on Computational Biology and Bioinformatics* (2019).

[7] Antonio Fabregat, Steven Jupe, Lisa Matthews, Konstantinos Sidiroopoulos, Marc Gillespie, Phani Garapati, Robin Haw, Bijay Jassal, Florian Korninger, Bruce May, et al. 2018. The reactome pathway knowledgebase. *Nucleic acids research* 46, D1 (2018), D649–D655.

[8] Yuchong Gong, Yanqing Niu, Wen Zhang, and Xiaohong Li. 2019. A network embedding-based multiple information integration method for the MiRNA-disease association prediction. *BMC bioinformatics* 20, 1 (2019), 1–13.

[9] Zhou Huang, Jiangcheng Shi, Yuanxu Gao, Chunmei Cui, Shan Zhang, Jianwei Li, Yuan Zhou, and Qinghua Cui. 2019. HMDD v3.0: a database for experimentally supported human microRNA–disease associations. *Nucleic acids research* 47, D1 (2019), D1013–D1017.

[10] Bo-Ya Ji, Zhu-Hong You, Li Cheng, Ji-Ren Zhou, Daniyal Alghazzawi, and Li-Ping Li. 2020. Predicting miRNA-disease association from heterogeneous information network with GraRep embedding model. *Scientific Reports* 10, 1 (2020), 1–12.

[11] Fangfang Jin, Huanhuan Hu, Ming Xu, Shoubin Zhan, Yanbo Wang, Huayong Zhang, and Xi Chen. 2018. Serum microRNA profiles serve as novel biomarkers for autoimmune diseases. *Frontiers in immunology* 9 (2018), 2381.

[12] Alexander Junge, Jan C Refsgaard, Christian Garde, Xiaoyong Pan, Alberto Santos, Ferhat Alkan, Christian Anthön, Christian von Mering, Christopher T Workman, Lars Juhl Jensen, et al. 2017. RAIN: RNA–protein association and interaction networks. *Database* 2017 (2017).

[13] Bogumił Kaczkowski, Elfar Torarinsson, Kristin Reiche, Jakob Hull Havgaard, Peter F Stadler, and Jan Gorodkin. 2009. Structural profiles of human miRNA families from pairwise clustering. *Bioinformatics* 25, 3 (2009), 291–294.

[14] Andreas Keller, Petra Leidinger, Andrea Bauer, Abdou ElSharawy, Jan Haas, Christina Backes, Anke Wendschlag, Nathalia Giese, Christine Tjaden, Katja Ott, et al. 2011. Toward the blood-borne miRNome of human diseases. *Nature methods* 8, 10 (2011), 841–843.

[15] V Naray Kim and Jin-Wu Nam. 2006. Genomics of microRNA. *TRENDS in Genetics* 22, 3 (2006), 165–173.

[16] Thomas N. Kipf and Max Welling. 2017. Semi-Supervised Classification with Graph Convolutional Networks. In *International Conference on Learning Representations (ICLR)*.

[17] Ana Kozomara and Sam Griffiths-Jones. 2010. miRBase: integrating microRNA annotation and deep-sequencing data. *Nucleic acids research* 39, suppl_1 (2010), D152–D157.

[18] Guanghui Li, Jiawei Luo, Qiu Xiao, Cheng Liang, and Pingjian Ding. 2018. Predicting microRNA-disease associations using label propagation based on linear neighborhood similarity. *Journal of biomedical informatics* 82 (2018), 169–177.

[19] Jin Li, Sai Zhang, Tao Liu, Chenxi Ning, Zhuoxuan Zhang, and Wei Zhou. 2020. Neural Inductive Matrix Completion with Graph Convolutional Networks for miRNA-disease Association Prediction. *Bioinformatics* (2020).

[20] Yang Li, Chengxiang Qiu, Jian Tu, Bin Geng, Jichun Yang, Tianzi Jiang, and Qinghua Cui. 2014. HMDD v2.0: a database for experimentally supported human microRNA and disease associations. *Nucleic acids research* 42, D1 (2014), D1070–D1074.

[21] Yi Lin, Yan Zeng, Fan Zhang, Lu Xue, Zan Huang, Wenxin Li, and Mingxiong Guo. 2013. Characterization of microRNA expression profiles and the discovery of novel microRNAs involved in cancer during human embryonic development. *PLoS one* 8, 8 (2013), e69230.

[22] Minghui Liu, Jingyi Yang, Jiacheng Wang, and Lei Deng. 2020. Predicting miRNA-disease associations using a hybrid feature representation in the heterogeneous network. *BMC Medical Genomics* 13, 10 (2020), 1–11.

[23] John S Mattick and Igor V Makunin. 2005. Small regulatory RNAs in mammals. *Human molecular genetics* 14, suppl_1 (2005), R121–R132.

[24] Søren Mørk, Sune Pletscher-Frankild, Albert Pallejà Caro, Jan Gorodkin, and Lars Juhl Jensen. 2014. Protein-driven inference of miRNA–disease associations. *Bioinformatics* 30, 3 (2014), 392–397.

[25] Xiaoyong Pan and Hong-Bin Shen. 2020. Scoring disease-microRNA associations by integrating disease hierarchy into graph convolutional networks. *Pattern Recognition* (2020), 107385.

[26] Sune Pletscher-Frankild, Albert Pallejà, Kalliopi Tsafou, Janos X Binder, and Lars Juhl Jensen. 2015. DISEASES: Text mining and data integration of disease-gene associations. *Methods* 74 (2015), 83–89.

[27] Juan José Rodriguez, Ludmila I Kuncheva, and Carlos J Alonso. 2006. Rotation forest: A new classifier ensemble method. *IEEE transactions on pattern analysis and machine intelligence* 28, 10 (2006), 1619–1630.

[28] Harpreet Kaur Saini, Sam Griffiths-Jones, and Anton James Enright. 2007. Genomic analysis of human microRNA transcripts. *Proceedings of the National Academy of Sciences* 104, 45 (2007), 17719–17724.

[29] R Schickel, B Boyerinas, SM Park, and ME Peter. 2008. MicroRNAs: key players in the immune system, differentiation, tumorigenesis and cell death. *Oncogene* 27, 45 (2008), 5959–5974.

[30] Lynn Maria Schriml, Cesar Arze, Suvarna Nadendla, Yu-Wei Wayne Chang, Mark Mazaitis, Victor Felix, Gang Feng, and Warren Alden Kibbe. 2012. Disease Ontology: a backbone for disease semantic integration. *Nucleic acids research* 40, D1 (2012), D940–D946.

[31] Eric M Small, Robert JA Frost, and Eric N Olson. 2010. MicroRNAs add a new dimension to cardiovascular disease. *Circulation* 121, 8 (2010), 1022–1032.

[32] Damian Szklarczyk, Andrea Franceschini, Stefan Wyder, Kristoffer Forslund, Davide Heller, Jaime Huerta-Cepas, Milan Simonovic, Alexander Roth, Alberto Santos, Kalliopi P Tsafou, et al. 2015. STRING v10: protein–protein interaction networks, integrated over the tree of life. *Nucleic acids research* 43, D1 (2015), D447–D452.

[33] Wataru Usuba, Fumihiro Urabe, Yusuke Yamamoto, Juntaro Matsuzaki, Hideo Sasaki, Makiko Ichikawa, Satoko Takizawa, Yoshiaki Aoki, Shumpei Niida, Ken Kato, et al. 2019. Circulating miRNA panels for specific and early detection in bladder cancer. *Cancer science* 110, 1 (2019), 408–419.

[34] Twan van Laarhoven, Sander B Nabuurs, and Elena Marchiori. 2011. Gaussian interaction profile kernels for predicting drug–target interaction. *Bioinformatics* 27, 21 (2011), 3036–3043.

[35] Dong Wang, Juan Wang, Ming Lu, Fei Song, and Qinghua Cui. 2010. Inferring the human microRNA functional similarity and functional network based on microRNA-associated diseases. *Bioinformatics* 26, 13 (2010), 1644–1650.

[36] Zhen Yang, Liangcai Wu, Anqiang Wang, Wei Tang, Yi Zhao, Haitao Zhao, and Andrew E Teschendorff. 2017. dbDEMC 2.0: updated database of differentially expressed miRNAs in human cancers. *Nucleic acids research* 45, D1 (2017), D812–D818.

[37] Xiangxiang Zeng, Wen Wang, Gaoshan Deng, Jiaxin Bing, and Quan Zou. 2019. Prediction of potential disease-associated microRNAs by using neural networks. *Molecular Therapy-Nucleic Acids* 16 (2019), 566–575.

[38] Wenyong Zhang, James E Dahlberg, and Wayne Tam. 2007. MicroRNAs in tumorigenesis: a primer. *The American journal of pathology* 171, 3 (2007), 728–738.

[39] Kai Zheng, Zhu-Hong You, Lei Wang, Yong Zhou, Li-Ping Li, and Zheng-Wei Li. 2020. DBMDA: A Unified Embedding for Sequence-Based miRNA Similarity Measure with Applications to Predict and Validate miRNA-Disease Associations. *Molecular Therapy-Nucleic Acids* 19 (2020), 602–611.